Journal of Applied Polymer Science

Separation of Lysozyme with Magnetically Stabilized Spherical Hydroxyapatite Microcomposites in a Continuous Flow System

Birnur Akkaya
Department of Molecular Biology and Genetics, Cumhuriyet University, Sivas 58140, Turkey
Correspondence to: B. Akkaya (E-mail: pergamonchem@gmail.com)

ABSTRACT: The aim of this study was to produce a spherical and magnetic hydroxyapatite (HA) microcomposite to use as an adsorbent for the separation of lysozyme in a magnetically stabilized fluidized bed and to separate lysozyme from a protein mixture composed of human immunoglobulin G, human serum albumin, and lysozyme. For this purpose, spherical and magnetic HA microcomposites (50–100 μm) were synthesized by suspension polymerization and characterized by Fourier transform infrared spectroscopy, X-ray diffraction, scanning electron microscopy, electron spin resonance, vibrating-sample magnetometry, Brunauer–Emmett–Teller analysis, and a swelling test. The specific surface areas of the pure HA and magnetic HA microcomposite were determined to be 72.25 and 151.53 m^2/g, respectively. The swelling ratio of the spherical HA microcomposites was 150%. Adsorption experiments were conducted under conditions that differed in terms of pH, temperature, ionic strength, flow velocity, and magnetic field. According to the findings of the adsorption kinetic studies, the adsorption process was appropriate to pseudo-first-order kinetics. The separation of the lysozyme from the protein mixture was achieved by means of a 50 m*M* pH 7.0 phosphate buffer. © 2013 Wiley Periodicals, Inc. J. Appl. Polym. Sci. 130: 1602–1610, 2013

KEYWORDS: biomaterials; biocompatibility; composites; proteins

Received 21 January 2013; accepted 10 March 2013; Published online 3 May 2013
DOI: 10.1002/app.39289

INTRODUCTION

Hydroxyapatite (HA) chromatography is considered to be a pseudo-affinity or mixed-mode ion-exchange chromatography technique. However, it differs from ion-exchange chromatography because of its elution process.[1] The protein purification with this method is mainly based on the interactions of the C side (calcium) of HA with the carboxyl groups of the related protein (metal affinity interaction) and the P side (phosphate) of HA with the amino groups of the related protein (cation exchange/interaction). Metal affinity interactions can be altered with ions with high calcium affinity, as cation-exchange interactions can be discarded with any salt.[2,3]

HA chromatography has been used for the chromatographic separation of proteins, nucleic acids, and antibodies over past decades.[4–6] Many HA support materials are used in columns, including crystalline, ceramic, and composite materials. HA Ultrogel sorbents (microcrystalline in agarose gel particles, Pall Corp.) and Bio-Gel HT HA (Bio-Rad Laboratories) were used for BSA adsorption. Many adsorption studies have been performed with lysozyme.[7–9]

Porous type I CHT adsorbed larger amounts of lysozyme compared with type II CHT because of its lower surface area.[10] Among these studies, only a limited number of systems use magnetic HA for protein separation in a magnetically stabilized fluidized bed (MSFB) system. One of these studies used BcMag HA modified magnetic beads in a batch mode.

Aside from these experiments, HA has received limited attention as a chromatographic material for protein purification because of its aggregation, the difficulty of predicting its chromatographic behavior, its low adsorption capacity, and challenges with its handling properties; this has resulted in a product that is not sufficiently pure. For most applications, other materials with superior chromatographic properties have been preferred. Because of the instability of the crystals, their applications in column system experiments are restricted. For this reason, materials that are porous, spherical and mechanically stable due to a high surface area are significant in producing hydroxyapatite,[11–13] which can be used in MSFB, which, in turn, enable a continuous countercurrent process. The use of MSFBs is an alternative to conventional column operations, such as packed beds or fluidized beds, especially for the large-scale purification of biological products. Magnetic stabilization enables the expansion of a packed bed without any mixing of solid particles. High column efficiency, a low pressure drop, and the elimination of clogging can be achieved.[14,15] Thus, MSFBs are suitable

© 2013 Wiley Periodicals, Inc.

for some applications in various areas, such as the separation of some biomolecules.[16] Many studies have compared MSFB systems and conventional operations for protein purification and the separation of biomolecules. Ding and Sun[17] compared the BSA adsorption capacity of magnetic pellicular supports for an MSFB and an expanded bed and found that the binding capacity in the MSFB was 60% higher than that in the expanded bed. Akkaya[18] compared the adsorption of immunoglobulin G (IgG) with magnetic poly(glycidyl methacrylate) [poly(GMA)] beads in batch mode and in an MSFB system and showed that adsorption in the MSFB system was higher than in the batchwise experiments. Because of the magnetic properties of the support materials in an external magnetic field, the removal of the adsorbed materials (target protein) can be easy and selective. The magnetic behavior makes the material easy to handle; therefore, the target protein can be removed from the protein mixture more efficiently. Magnetic separation in an MSFB can facilitate the separation and purification processes.[19,20] Tong and Sun[21] prepared a magnetic agarose support in an MSFB for lysozyme adsorption and compared the adsorption capacity of lysozyme in the MSFB (55.8 mg of lysozyme/g of support) to that in an expanded bed (31.1 mg of lysozyme/g of support) at a liquid velocity of 45 cm/h.

The minimum number of magnetic particles needed to stabilize the bed is calculated as a function of various parameters, including the size, magnetic field strength, and fluidization velocity. A variety of commercially available affinity, ion-exchange, and adsorptive supports can be used for continuous countercurrent separation in the bed.[22,23]

Different methods have been developed to separate lysozymes. These methods include ultrafiltration (Ghosh et al.[24] used hollow-fiber ultrafiltration for lysozyme separation studies), metal chelate affinity chromatography [Şenel et al.[25] used Cu-chelated p(2-hydroxyethylmethacrylate-methacrylamidohistidine) [p(HEMA–MAH)] beads], membrane separation {Arıca and Bayramoğlu[26] used a dye-ligand-immobilized affinity membrane [RR-120 p(hydroxyethylmethacrylate) [p(HEMA)]/chitosan[26]}, and ion-exchange chromatography (Safarik et al.[27] used magnetic macroporous cellulose cation exchangers for lysozyme separation). However, the severe limitations of many of these methods, including long processing steps, high cost, and dilution of egg white during processing, have hampered their applications.

In this study, magnetic and spherical HA microcomposites were prepared by suspension polymerization in the presence of HA, ethylene glycol dimethacrylate (EGDMA), poly(vinyl alcohol) (PVA), magnetite (Fe_3O_4), and benzoyl peroxide (BPO). The adsorption of lysozyme on magnetic–spherical hydroxyapatite microcomposites (m–s HA) in aqueous media (in an MSFB system) was investigated at different lysozyme concentrations, ionic strengths, pH levels, flow velocities, magnetic fields, and temperatures. The m–s HA microcomposites were characterized with Fourier transform infrared (FTIR), electron spin resonance (ESR), and X-ray diffraction (XRD) spectroscopy; scanning electron microscopy; vibrating-sample magnetometry (VSM); Brunauer–Emmett–Teller (BET) analysis; and a swelling test system. The desorption of lysozyme and the reusability of the HA microcomposites were also tested.

EXPERIMENTAL

Chemicals

Lysozyme (lyophilized and from chicken egg white) and EGDMA were obtained from Fluka (Buchs, Switzerland). BPO was also obtained from Fluka. PVA (molecular weight = 85.000–140.000, 98% hydrolyzed), magnetite (Fe_3O_4), and pure HA were supplied from Sigma-Aldrich (Steinheim, Germany). Buffer solutions were prefiltered through a 0.2-μm membrane (Whatman, Dassel, Germany). All glassware was washed extensively with diluted nitric acid before use. All other chemicals were of analytical-grade purity and were purchased from Merck (Darmstadt, Germany).

Synthesis of the Magnetic and Spherical HA Microcomposites

The magnetic and spherical HA microcomposites were prepared under suspension polymerization. The following experimental procedure was applied for the synthesis of the spherical HA microcomposites: 200 mg of PVA (the stabilizer) was dissolved in 50 mL of deionized water for the preparation of the continuous phase. For the dispersion phase, 8.0 mL of EGDMA (the crosslinker), 1.0 g of HA powder, 1.0 g of magnetite (Fe_3O_4), and 12.0 mL of toluene (as a pore maker) were mixed in a beaker. An amount of 100 mg of BPO (the initiator) was dissolved in this homogeneous solution. The dispersion phase was added to the continuous medium in a glass-sealed polymerization reactor (100 mL), which was placed in a water bath equipped with a temperature-control system. The polymerization reactor was heated to 65°C, and the polymerization medium was stirred at 500 rpm for 4 h. At the end of the polymerization, the reactor content was cooled at room temperature. To remove the diluent, any possible unreacted monomer, and other ingredients from the beads, a washing procedure was followed after polymerization. The suspension was stirred for approximately 1 h at room temperature, and the beads were separated by filtration. When not in use, to prevent microbial contamination, the beads were refrigerated in a 0.02% sodium azide solution.

Characterization of the Magnetic and Spherical HA Microcomposites

The surface area of the m–s HA microcomposite was determined by means of the BET equation with a nitrogen adsorption system at 77 K; this was determined with a Quantachromosorb instrument. The average size and size distribution of the samples were determined via a screen analysis performed with standard test sieves (Retsch GmbH and Co., Germany). The water-uptake ratios of the pure and magnetic and spherical HA microcomposites were determined in distilled water. The water content of the m–s HA microcomposite was calculated with the weights of the microcomposites before and after the uptake of water. The surface morphology of the m–s HA microcomposites was examined with a scanning electron microscope (model JSM 5600, JEOL, Japan).

For the chemical structure characterization of the pure HA, magnetite, and m–s HA microcomposites, FTIR spectra were obtained with an FTIR spectrophotometer (Mattson 1000, United Kingdom). To determine the power diffractions of the pure HA, magnetite, and m–s HA microcomposites, XRD was

performed on a Rigaku Dmax 2200 with Cu Kα radiation at a 2θ scan rate per minute. The presence of magnetite particles in the polymeric structure was investigated with an ESR spectrometer (EL 9, Varian, Chicago). The magnetization curve of the m–s HA microcomposites was obtained from a VSM instrument [Cryogenic, Ltd., Physical Property Measurement System (PPMS®)].

Adsorption of Lysozyme from Aqueous Solutions

The adsorption capacity of the m–s HA microcomposite for lysozyme was determined in an MSFB system by means of a Bio-Rad economic column (diameter = 1.0 cm, length = 10.0 cm) surrounded by a magnetic field generator [root-mean-square value of the magnetic field (B_{rms}) ≈ 24 G, peak to peak value of the magnetic field (B_{p-p}) ≈ 33 G, magnetic flux (ϕ) = 50 Hz). The flow of lysozyme solution through the column was enabled with an ALITEA (Sweden) peristaltic pump. The m–s HA microcomposites were incubated with 25 mL of lysozyme solution for 2 h under a magnetic field. The effects of the time, pH, temperature, ionic strength, flow rate, and magnetic field on the adsorption capacity were studied. To observe the effects of the initial concentration of lysozyme on adsorption, the initial concentration was varied between 0.5 and 2.5 mg/mL. Lysozyme adsorption was investigated within a range of pH from 5.0 (acetate buffer) and to 6.0–8.0 (phosphate buffer). The effects of the temperature were tested at 15, 25, and 35°C. The effects of the ionic strength were studied in the range of 0.01–0.1*M* in an NaCl medium. The effects of the flow rate were investigated within the range 1–4.5 mL/min. The effects of the magnetic field were investigated with magnetic fields ranging between 6 and 20 mT. In all of the experiments, 0.1 g of particles was used. The adsorbed protein concentration was determined spectrophotometrically by the measurement of the absorbance at 280 nm. The amount of adsorbed lysozyme per m–s HA microcomposite was calculated with the concentrations of lysozyme in the initial solution and at equilibrium.

Desorption and Repeated Use

The desorption of lysozyme from the m–s HA microcomposites was performed in a 1.0*M* NaCl solution. The desorption agent was passed through the column containing the lysozyme-adsorbed m–s HA microcomposites for 1 h at room temperature. The final lysozyme concentration within the desorption medium was determined spectrophotometrically. The recovery was calculated from the amount of lysozyme adsorbed on the m–s HA microcomposites and the amount of lysozyme desorbed. Lysozyme adsorption–desorption cycles were performed 10 times with the same m–s HA microcomposites to test the reusability of the m–s HA microcomposites.

Separation of Lysozyme from the Protein Mixture

The 10-mL mixture containing human serum albumin (HSA; 1.5 mg/mL), human γ-globulin (1.5 mg/mL), and lysozyme (1.5 mg/mL) was pumped through the m–s HA microcomposite column with a peristaltic pump for 2 h (at 25°C, a pH of 7.0 in 50 m*M* phosphate buffer, and a 1.0 mL/min flow rate). During the experiments, the magnetic microcomposites in the column were exposed to a magnetic field. The total protein concentration was measured with a 280-nm ultraviolet–visible spectrophotometer. Elution was performed with a 0.5*M* NaCl solution.

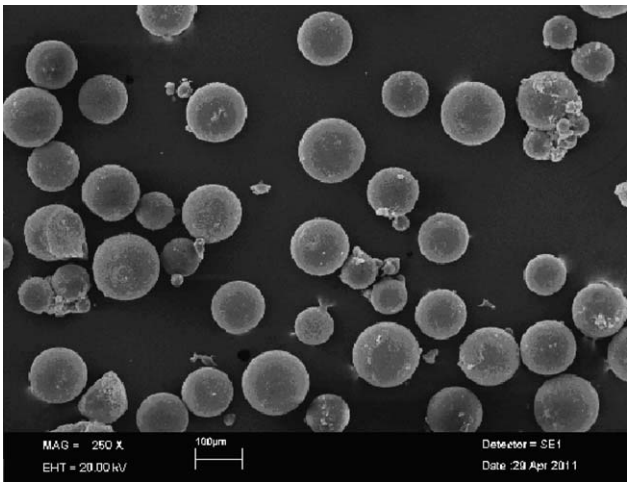

Figure 1. Scanning electron micrograph of the m–s HA microcomposite.

Lysozyme separation (adsorption and desorption) was assayed with sodium dodecyl sulfate–polyacrylamide gel electrophoresis (SDS–PAGE) and a 10% separating gel; 4% stacking gels were stained with 0.25% Coomassie Brilliant R 250 in an acetic acid–methanol–water (1:5:5 v/v/v) mixture and were destained in an ethanol–acetic acid–water (1:4:6 v/v/v) mixture.

RESULTS AND DISCUSSION

Properties of the Magnetic and Spherical HA Microcomposites

The m–s HA microcomposites were obtained by the crosslinking of Fe_3O_4 powder (organic material) and HA (inorganic material). The microcomposites did not dissolve in aqueous media, but they did swell, depending on the degree of crosslinking. The equilibrium swelling ratio of the m–s HA was 150%. Compared with pure HA (60%), the water-uptake ratio of the m–s HA microcomposites increased because of the incorporation of the organic material.

The radical suspension polymerization procedure provided crosslinked m–s HA in the size range of 50–100 μm in diameter (diameter of pure HA < 200 nm). The BET surface areas of the pure and m–s HA were 72.25 and 151.53 m^2/g, respectively; the surface area thus increased in the microcomposites. This increase in surface area provided the adsorbent with high protein adsorption features. We concluded that m–s HA had a sufficient surface area and pore size (30 nm) for the separation of lysozyme in the MSFB system compared with the nonporous and nonspherical pure HA.

The size and surface morphology of the m–s HA are shown in the scanning electron micrographs presented in Figure 1. As is clearly shown, the m–s HA microcomposites had a spherical form and a rough surface because of the pores that were formed during the polymerization procedure. The roughness of the

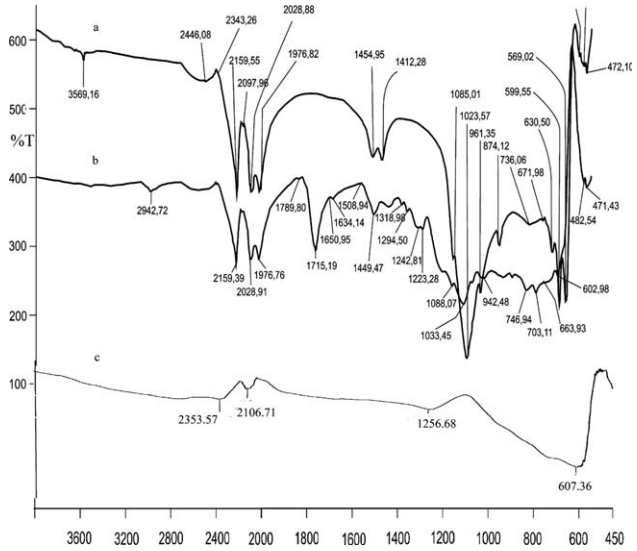

Figure 2. FTIR spectra of the (a) pure HA, (b) magnetic HA microcomposite, and (c) Fe_3O_4.

surface should be considered a contributing factor to the increase in the surface area.

Figure 2 shows the FTIR spectrum of the pure HA, m–s HA microcomposites, and Fe_3O_4 nanopowder. In Figure 2(a), the peaks at 602, 962, and 1035 cm^{-1} are typical frequencies of the PO_4 groups of HA, and also, the sharp band at 3500 cm^{-1} shows —OH stretching.[28,29] When the m–s HA microcomposites' FTIR spectra were compared with those of pure HA and Fe_3O_4, the modifications could be clearly seen. With the incorporation of EGDMA in the structure, extra peaks between 1600 and 1750 cm^{-1} because of to the carbonyl stretching of EGDMA. In addition, there were also C—H bending bands in the frequency range of 1200–1400 cm^{-1}.

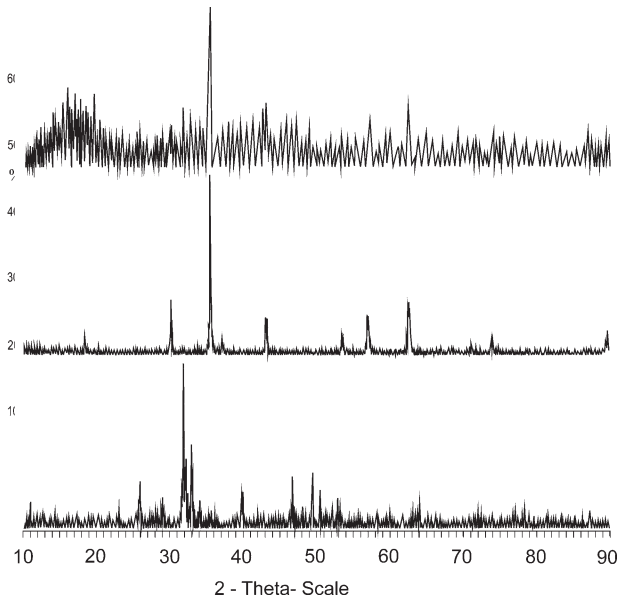

Figure 3. XRD patterns of the (a) Fe_3O_4, (b) pure HA, and (c) magnetic HA microcomposite.

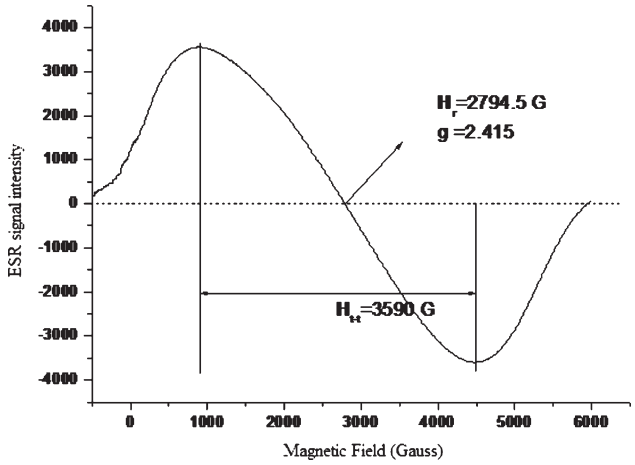

Figure 4. ESR spectrum of the m–s HA microcomposite.

Figure 3 shows the XRD patterns of the magnetite (Fe_3O_4), pure HA, and porous spherical HA microcomposites. As shown in Figure 3(b,c), all of the peaks were typical for HA ($2\theta = 26$, 32, and 34°). Compared with the peaks in Figure 3(b), peak broadening was due to the amorphous contribution of organic material (EGDMA; $2\theta = 16°$).[30,31] The main peak of Fe_3O_4 magnetite also appeared in the XRD spectrum [$2\theta = 16°$; Figure 3(a)].

The presence of magnetite particles in the microcomposite structure was confirmed via ESR spectroscopy, with the corresponding spectrum showing the intensity of the magnetite peak against the magnetic field (gauss), as depicted in Figure 4. The H_r value is defined as the external magnetic field at resonance. The application of an external field can generate an internal magnetic field in the sample that can add to or subtract from the external field. The local magnetic field generated by the electronic magnetic moment will add vectorially to the external magnetic field and result in an effective field. The m–s HA microcomposites had a relative intensity of approximately 250 and exhibited a local magnetic field because of the magnetite contained within that structure. The g value is a valuable factor. In the literature, the g factor ranges between 1.4 and 3.1.[32] In this study, the g factor was found to be 2.415 for the m–s HA microcomposites.

The magnetic properties of the polymeric structure are also presented in terms of the electron mass unit in Figure 5, which shows the behavior of the magnetic beads in a magnetic field generated by a vibrating magnetometer. In the electron mass unit spectrum and from the effective magnetic field value [Tesla (T) = 10^4 Gs], a 2794.5-G magnetic field was found to be sufficient to excite all of the dipole moments present in a 1.0-g sample of the m–s HA microcomposite. This value is an important design parameter for an MSFB or for magnetic filtration with these beads. The value of this magnetic field is a function of the flow velocity, particle size, and magnetic susceptibility of the solids to be removed. In the literature, this value has been found to vary between 8 and 20 kG for various applications;[33] thus, the magnetic beads in this study required a lower

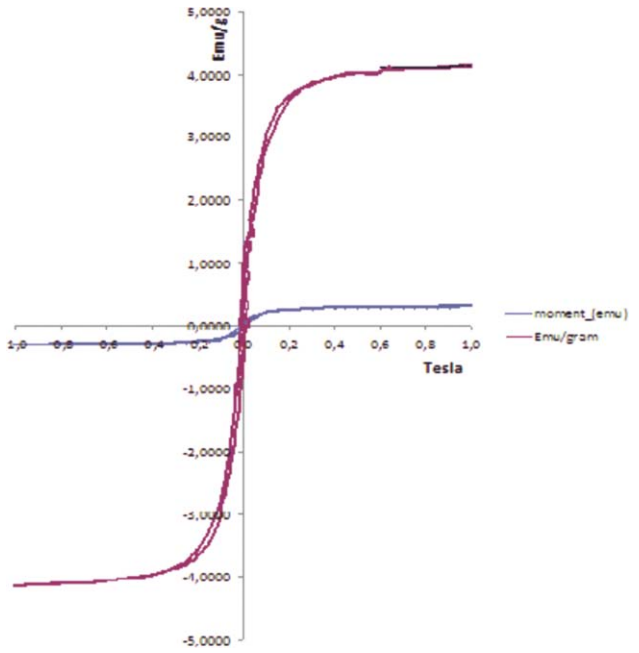

Figure 5. Magnetic hysteresis curves (VSM) of the m–s HA microcomposite. [Color figure can be viewed in the online issue, which is available at wileyonlinelibrary.com.]

magnetic intensity in an MSFB, as reported in another study.[34] As shown in the magnetization curve (Figure 5), because of the extremely low coercive forces[35] and zero remanence (when the external magnetic field was zero, the magnetization was also zero),[17] the m–s HA could be regarded as superparamagnetic; this means that the m–s HAs would not interact with one another and would not agglomerate after the external magnetic field was removed.[36]

Adsorption Studies

Effect of the Time and Adsorption Kinetics Modeling. Lysozyme adsorptions were carried out at different contact times with various initial lysozyme concentrations (0.5–2.5 mg/mL). Figure 6 shows the effect of the contact time on the adsorption capacity at different initial lysozyme concentrations. The maximum adsorption capacity was clearly reached after 60 min (up to 120 mg/g) at the initial lysozyme concentration of 2 mg/mL. The initial increase was observed within the first 15 min. This behavior of the adsorption process was due to the fact that the m–s HA microcomposites had a large number of interaction sites for the lysozyme. Later, the adsorption capacity decreased because of the saturation of the interaction sites and the decrease in the lysozyme concentration.[27,37]

The adsorption process was examined with kinetic models to test the experimental data. Pseudo-first- and pseudo-second-order equations could be used in this case, with the assumption of the formation of a monolayer. The Lagergren model is among the most widely used for the adsorption of solute from a liquid solution.[38]

It may be represented as follows:

$$dqt/dt = k_1(q_e - q_t) \quad (1)$$

where k_1 is the rate constant of the pseudo-first-order adsorption (1/min) and q_e and q_t denote the amounts of adsorbed protein at equilibrium and at time t (mg/g), respectively. After integration, the application of boundary conditions ($q_t = 0$ at $t = 0$ and $q_t = q_t$ at $t = t$) yields

$$\log[q_e/(q_e - q_t)] = (k_1 t)/2.303 \quad (2)$$

Equation (2) can be rearranged into the following linear form:

$$\mathrm{Log}\,(q_e - q_t) = \log q_e - k_1 t/2.303 \quad (3)$$

A plot of $\log(q_e - q_t)$ versus t should result in a straight line to confirm the applicability of the kinetic model. In a true first-order process, log q_{eq} should equal the interception point of a plot of $\log(q_e - q_t)$ versus t. In addition, a pseudo-second-order equation based on the equilibrium adsorption capacity may be expressed in the following form:

$$t/q_t = 1/kq_e^2 = \quad (1/q_e)\mathrm{t} \quad (4)$$

A plot of t/q_t versus t should yield a linear relationship in terms of the applicability of second-order kinetics. The rate constant (k_2) and q_e can be obtained from the intercept and slope, respectively. A comparison of the experimental adsorption capacity (Q_{eq}) and the theoretical values (q_e) is presented in Table I. The theoretical q_e values estimated from the pseudo-first-order kinetic model were very close to the experimental values, and the correlation coefficients were higher than those determined from the pseudo-second-order model. These results suggest that the pseudo-first-order mechanism was predominant, as indicated in the literature.[39] We concluded that the lysozyme corresponded to the monolayer on the surface of HA, as reported in a previous work.[40]

Effects of the pH, Temperature, and Ionic Strength. The adsorption of lysozyme on the m–s HA microcomposite as a function of pH (pH = 5.0–8.0) is shown in Figure 7(a). The amount of adsorbed lysozyme reached a maximum at pH 7.0

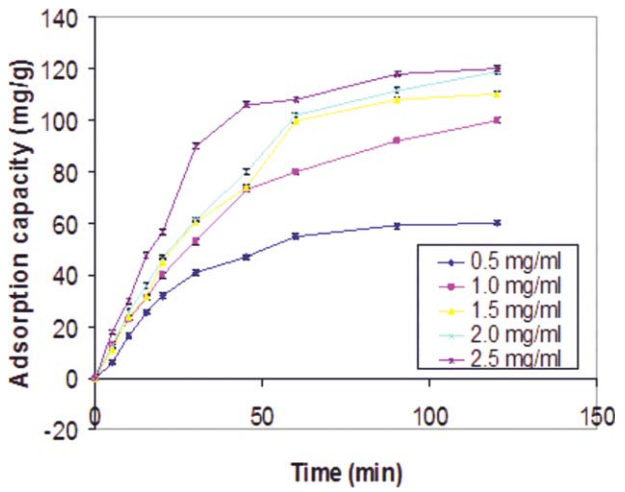

Figure 6. Effect of the lysozyme concentration on the lysozyme adsorption: pH 7.0 (50 m*M* phosphate buffer), temperature = 25°C, $B = 6$ mT, and flow rate = 1 mL/min. [Color figure can be viewed in the online issue, which is available at wileyonlinelibrary.com.]

Table I. Results of the Kinetic Studies

Pseudo-first-order study				Pseudo-second-order study		
Q_{eq} (mg/g)	k_1 (min^{-1})	q_e (mg/g)	R^2	k_2 (g mg^{-1} min^{-1})	q_e (mg/g)	R^2
120	0.0454	133.66	0.9848	1.736×10^{-4}	163.93	0.9661

(in 50 m*M* phosphate buffer), with decreases at lower and higher pH values. The pH is an important parameter in the adsorption process because it affects the ionization state of the protein and the surface charge of the adsorbent being used.[39] The surface of the m–s HA microcomposites had a mosaic of positive (calcium) and negative (phosphate) sites. Since HA columns are normally operated at pH 6.8 after extensive washing with a phosphate buffer, the surface of the column can be regarded as negative because of a partial neutralization of the positive calcium loci by phosphate ions.[10]

Lysozyme is a basic protein (p*I* = 11.0). In the adsorption medium (50 m*M* at pH 7.0 in phosphate buffer), the protein surface will be positively charged, and the adsorbent surface will be negatively charged. The presence of phosphate ions will cover the surface of the adsorbent because they will interact with Ca^{2+} ions. This could eliminate the electrostatic repulsions between the positive groups of protein and Ca^{2+} ions. At this pH value, therefore, positively charged lysozyme could interact more easily with the m–s HA surface.

The effect of the temperature on the adsorption of lysozyme on m–s HA was studied at various temperatures (15, 25, and 35°C). As shown in Figure 7(b), with increasing temperature, the adsorbed lysozyme per m–s HA microcomposite increased. The adsorption process was endothermic.[41,42] The increase in the adsorption capacity was due to conformational changes in the lysozyme. High temperatures provided more available side chains for interactions with the surface of m–s HA.[43]

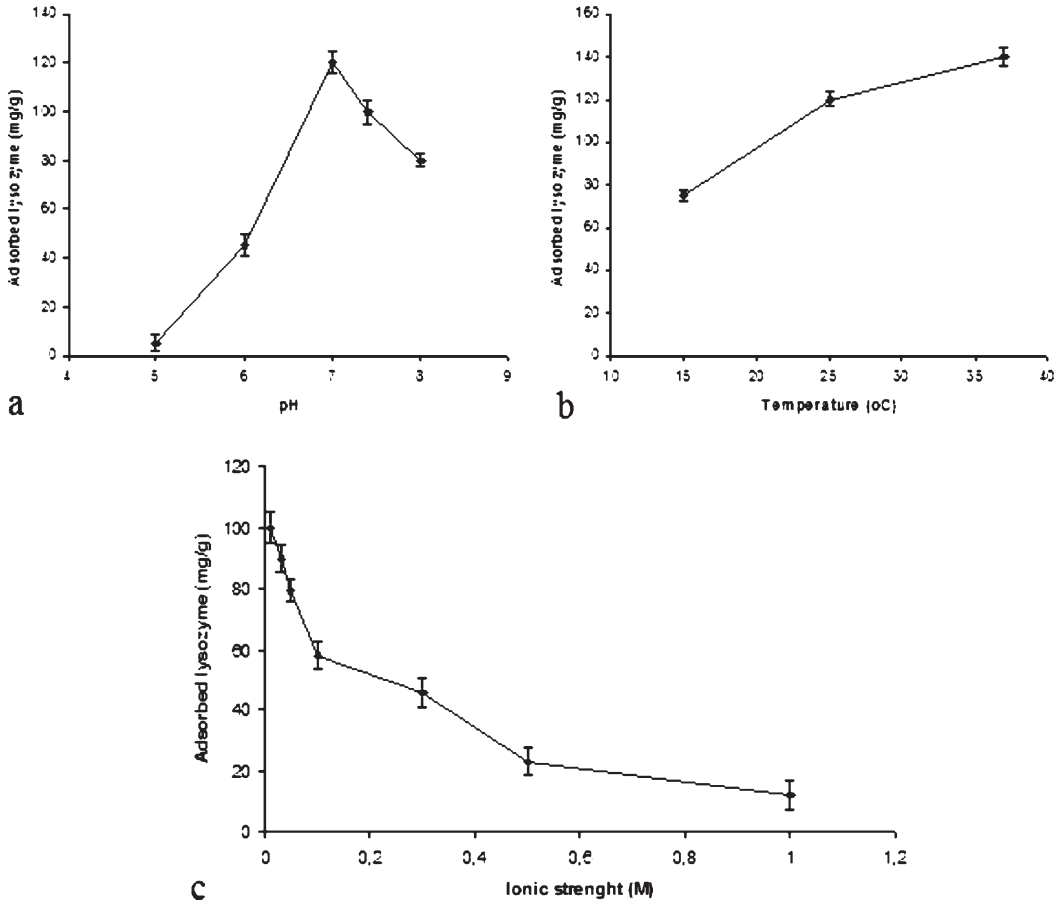

Figure 7. (a) Effect of pH on the lysozyme adsorption (lysozyme concentration = 2.0 mg/mL, temperature = 25°C, flow rate = 1 mL/min, and $B = 6$ mT), (b) effect of the temperature on the lysozyme adsorption (pH = 7.0, lysozyme concentration = 2.0 mg/mL, flow rate = 1 mL/min, and $B = 6$ mT), and (c) effect of the ionic strength on the lysozyme adsorption (pH = 7.0, lysozyme concentration = 2.0 mg/mL, temperature = 25°C, flow rate = 1 mL/min, and $B = 6$ mT). All of the experiments were performed in triplicate.

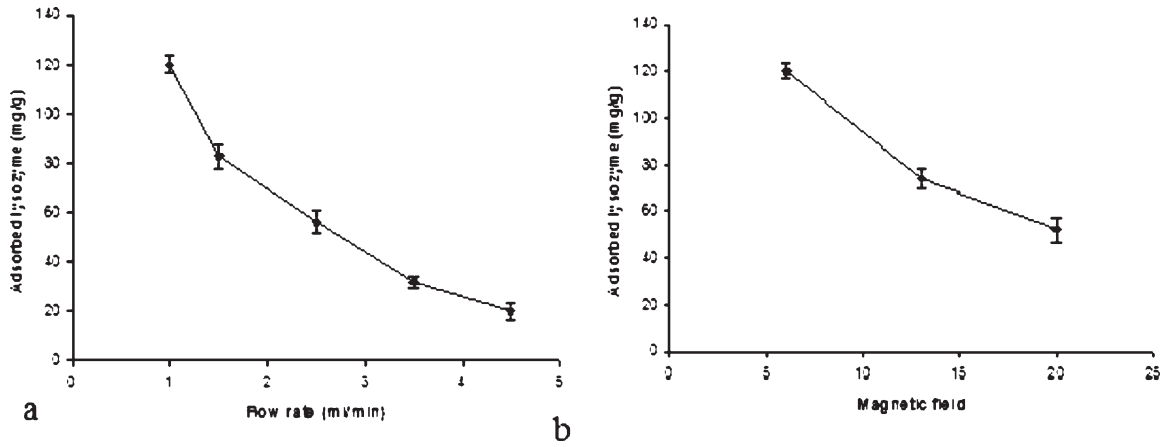

Figure 8. (a) Effect of the flow rate on the adsorption capacity (pH = 7.0, lysozyme concentration = 2,0 mg/mL, temperature = 25°C, and $B = 6$ mT) and (b) effect of the magnetic field on the adsorption capacity (pH = 7.0, lysozyme concentration = 2,0 mg/mL, temperature = 25°C, and flow rate = 1 mL/min). All of the experiments were performed in triplicate.

The effect of the ionic strength on the lysozyme adsorption is presented in Figure 7(c). The adsorption capacity decreased with increasing ionic strength. Lysozyme adsorption on the m–s HA microcomposite decreased by approximately 90%, whereas the concentration of NaCl changed from 0.01 to 1.0*M*. The presence of Na^+ and Cl^- ions in the medium may have caused a change in the adsorption of amino acids on the m–s HA microcomposites. The decrease in the adsorption capacity as the ionic strength increased may have been due to decreasing ion-exchange interactions[44] between the m–s HA microcomposites and lysozyme molecules.

Effect of the Flow Rate and Effect of the Magnetic Field. The lysozyme adsorption capacity of the m–s HA microcomposites at different flow rates is shown in Figure 8(a). The adsorption capacity decreased from 120 to 20 mg/g with an increase in the flow rate from 1.0 to 4.5 mL/min. Because of the long contact time in the column with decreasing flow rate, the lysozyme had more time to interact with the m–s HA microcomposite; hence, a better adsorption capacity was obtained.[45] The effect of the flow rate demonstrated that the binding was kinetically limited, and the kinetically limited binding was supported by a smaller thickness in terms of the diffusion layer as thickness of the diffusion layer depended on the flow velocity of the sample.[46] Thus, the sample uptake rate was achieved, and this determined the residence time required for the completion of the adsorption reaction.[47]

As seen in Figure 8(b), when the magnetic field increased, the amount of adsorbed lysozyme decreased. Increasing the magnetic field led to a strong agglomeration of the magnetic particles and made the fluidization of the particles more difficult.[48]

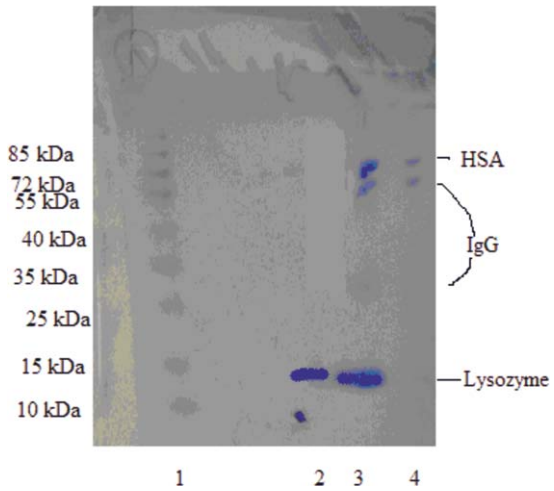

Figure 9. SDS–PAGE analysis of the lysozyme separation. Line 1: molecular weight marker, line 2: desorbed lysozyme, line 3: protein mixture before adsorption, and line 4: protein mixture after adsorption. [Color figure can be viewed in the online issue, which is available at wileyonlinelibrary.com.]

Separation of Lysozyme from the Protein Mixture with the m–s HA Microcomposites. As observed in the SDS–PAGE analysis, with a 50 m*M* pH 7.0 phosphate buffer medium, the m–s HA microcomposites could interact only with lysozyme. At this pH value, albumin (p$I = 4.7$) had negative amino acid residues

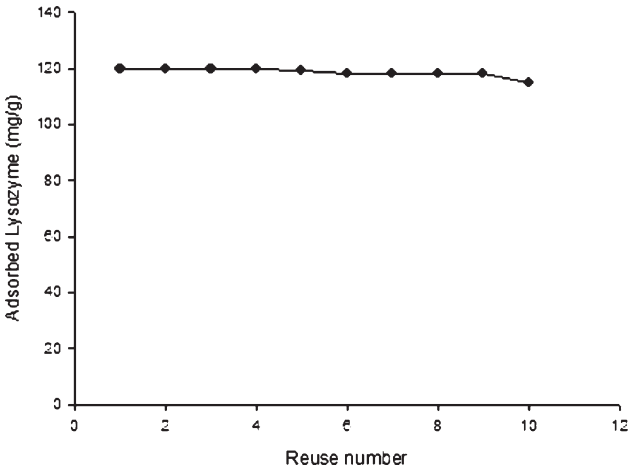

Figure 10. Reusability of the m–s HA microcomposite.

and could not be adsorbed by m–s HA. IgG (p$I = 6.2$) used both the C and P sites for interaction with m–s HA in pH 7.0 phosphate buffer (5–10 m*M* concentration). The difference was obvious in the SDS–PAGE results (Figure 9). With appropriate conditions (adsorption in the 50 m*M* pH 7.0 phosphate buffer and elution in the 0.5*M* NaCl medium), the m–s HA microcomposites showed good performance for lysozyme adsorption/desorption, as they did in other reported research.[49,50]

Desorption and Repeated Use

In this study, more than 97% of the adsorbed lysozyme molecules were desorbed easily from the m–s HA microcomposites during the 1 h when sodium chloride was used as a desorption agent in the 5 m*M* pH = 7.0 phosphate medium (Figure 10). The desorption of lysozyme from the m–s HA microcomposites was performed in an MSFB system. On the basis of the desorption graph (Figure 10), we concluded that NaCl was a suitable desorption agent for the desorption of lysozyme from the m–s HA microcomposites.[3] To demonstrate the reusability of the m–s HA microcomposites, the adsorption/desorption cycle was repeated 10 times with the same m–s HA microcomposite from an aqueous lysozyme solution (Figure 10). There was no significant loss in the adsorption capacity of the beads after 10 cycles.

CONCLUSIONS

A great deal of research has been reported pertaining to HA synthesis and its applications.[51–53] In this study, lysozyme was separated from the protein mixture (50 m*M* pH 7.0 phosphate buffer) and desorbed from the m–s HA microcomposites with 0.5*M* NaCl. These particles could be used efficiently for protein adsorption in a continuous countercurrent system because of their flow properties, magnetic properties, porous surface, high surface area, and spherical form. The introduction of all of these properties to pure HA caused the separation of the lysozyme multiple times with the same microcomposite. Thus, this newly synthesized material offered high lysozyme separation.

ACKNOWLEDGMENTS

This work was supported by The Research Fund of Cumhuriyet University (CÜBAP, project number F-323).

REFERENCES

1. Aizawa, T.; Kogenesawa, N.; Kamakura, A.; Masaki, K.; Matsuura, A.; Nagadome, H.; Terada, Y.; Kawano, K.; Nitta, K. *FEB Lett.* **1998**, *422*, 175.
2. Gagno, P. *Genet. Eng. N.* **2010**, *30*(7), 28.
3. Gagnon, P. N. *Biotechnology* **2009**, *25*(5), 287.
4. Yin, G.; Liu, Z.; Zhan, J.; Ding, F. X.; Yuan, N. *J. Chem. Eng. J.* **2002**, *87*, 181.
5. Kandori, K.; Mukai, M.; Yasukawa, A.; Ishikawa, T. *Langmuir* **2000**, *16*, 2301.
6. Figueiredo, K. C. D.; Salim, V. M. M.; Alves, T. L. M.;. Pinto, J. C. *Adsorption* **2005**, *11*, 131.
7. Barroug, A.; Lemaitre, J.; Rouxhet, P. G. *Colloid Surf. B* **1989**, *37*, 339.
8. Kawasaki, K.; Kambara, M.; Matsumura, H. *Colloid Surf. B* **2003**, *32*, 321.
9. Shi, X. L.; Feng, M. Q.; Shi, J. H.; Shi, J.; Zhong, J.; Zhou, P. *Protein Expression Purif.* **2007**, *54*, 24.
10. Cummings, L. J.; Snyder, M. A.; Brisack, K. *Methods Enzymol.* **2009**, *463*, 387.
11. Zhu, X. D.; Fan, H. S.; Zhao, C. Y.; Lu, J.; Ikoma, T.; Tanaka, J.; Zhang, X. D. *J. Mater. Sci. Mater. Med.* **2007**, *18*, 2243.
12. Komlev, V. S.; Barinov, S. M.; Koplik, E. V. *Biomaterials* **2002**, *23*, 3449.
13. Fujii, S.; Okada, M.; Furuzono, T. *J. Colloid Interface Sci.* **2007**, *315*, 287.
14. Lochmuller, C. H.; Ronsick, C. S.; Wigman L. S.; *Prep. Chromatogr.* **1988**, *1*, 93.
15. Burns, M. A.; Graves, D. *J. Biotechnol. Prog.* **1985**, *1*, 95.
16. Karataş, M.; Akgöl, S.; Yavuz, H.; Say, R.; Denizli, A. *Int. J. Biol. Macromol.* **2006**, *40*, 254.
17. Ding, Y.; Sun, Y. *Chem. Eng. Sci.* **2005**, *60*, 917.
18. Akkaya, B. Ph.D. Thesis, University of Cumhuriyet, **2009**.
19. Safarikova, M.; Safarik, I. *Magn. Electr. Sep.* **2001**, *10*, 223.
20. Safarik, I.; Safarikova, M. *Biomagn. Res. Technol.* **2004**, *2*, 7.
21. Tong, X. D.; Sun, Y. *Biotechnol. Progr.* **2003**, *19*, 1721.
22. Yılmaz, F.; Bereli, N.; Yavuz, H.; Denizli, A. *Biochem. Eng. J.* **2009**, *43*, 272.
23. Akkaya, B.; Yavuz, H.; Candan, F.; Denizli, A. *J. Appl. Polym. Sci.* **2012**, *125*, 1867.
24. Ghosh, R.; Silva, S. S.; Cui, Z. F. *Bio. Chem. Eng. J.* **2000**, *6*, 19.
25. Serap, S.; Elmas, B.; Camlı, T.; Andac, M.; Denizli, A. *Sep. Sci. Technol.* **2004**, *39*, 3783.
26. Arıca, M. Y.; Bayramoglu, G. *Process. Biochem.* **2005**, *40*, 1433.
27. Safarik, I.; Sabatkova, Z.; Tokar, O.; Safarikova, M. *Food Technol. Biotechnol.* **2007**, *45*, 355.
28. Ulusoy, U.; Akkaya, R. *J. Hazard. Mater.* **2009**, *163*, 98.
29. Sharpe, J. R.; Sammons, R. L.; Marquis, P. M. *Biomaterials* **1997**, *18*, 471.
30. Qiu, X.; Han, Y.; Zhuang, X.; Chen, X.; Li, Y.; Jing, X. *J. Nanopart. Res.* **2007**, *9*, 901.
31. Bundela, H.; Bajpai, A. K. *Express Polym. Lett.* **2008**, *2*, 201.
32. Swartz, H. M.; Bolton, J. R.; Borg, D. C. Biological Application of Electron Spin Resonance; Wiley: New York, **1972**.
33. Wang, Y. M.; Wang, Y. X.; Feng, L. X. *J. Appl. Polym. Sci.* **1997**, *64*, 1843.
34. Odabaşı, M. *Prep. Biochem. Biotechnol.* **2011**, *41*, 287.
35. Wang, D.; Duan, X.; Zhang, J.; Yao, A.; Zhou, L.; Huang, W. *J. Mater. Sci.* **2009**, *44*, 4020.
36. Tseng, J. Y.; Chang, C. Y.; Chen, Y. H.; Chang, C. F.; Chiang, P. C. *Colloid Surf. A* **2007**, *295*, 209.
37. Arıca, M. Y.; Bayramoğlu, G. *Process. Biochem.* **2005**,*40*, 1433.
38. Ho, Y. S.; McKay, G. *Process. Saf. Environ.* **1998**, *76*, 332.
39. Moradi, O.; Zare, K. *J. Phys. Theor. Chem. IAU Iran* **2011**, *7*, 263.

40. Kandori, K.; Mukai, M.; Fujiwara, A. *J. Colloid Interface Sci.* **1997**, *191*, 498.

41. Lin, Y. L.; Wang, R.; Ma, W.; Cheng, Z. H. *Adv. Mater. Res.* **2011**, *343*, 909.

42. Chen, X.; Liu, J.; Feng, Z.; Shao, Z. *J. Appl. Polym. Sci.* **2005**, *96*, 1267.

43. Lu, A. X.; Liao, X. P.; Zhou, R. Q.; Shi, B. *Colloid Surf. A* **2007**, *301*, 85.

44. Gagnon, P.; Cheung, C. W.; Yazaki, P. J. *J. Sep. Sci.* **2009**, *32*, 3857.

45. Valdman, E.; Erijman, L.; Pessoa, F. L. P.; Leite, S. G. F. *Process. Biochem.* **2001**, *36*, 869.

46. Lange, K.; Griffin, G.; Vo-Dinh, T.; Gauglitz, G. *Talanta* **2002**, *56*, 1153.

47. Hui, Q. I. U.; Lu, L. V.; Bing-Cai, P.; Qing-Jian, Z.; Wei-Ming, Z.; Quan-Xing Z. *J Zhejiang Univ. Sci. A* **2009**, *10*, 716.

48. Böhm, D.; Pittermann, B. *Chem. Eng. Technol.* **2000**, *23*, 4.

49. Anirudhan, T. S.; Rejeena, S. R. *Chem. Eng. J.* **2012**, *187*, 150.

50. Garcia-Diego, C.; Cuellar, J. *Chem. Eng. J.* **2008**, *143*, 337.

51. Zhou, H.; Lee, J. *Acta Biomater.* **2011**, *7*, 2769.

52. Dasgupta, S.; Bandyopadhyay, A.; Bose, S. *Acta Biomater.* **2009**, *5*, 3112.

53. Ng, S.; Guo, J.; Ma, J.; Loo, S. C. *J. Acta Biomater.* **2010**, *6*, 3772.